



Biosorption applications of lichen *Pseudevernia furfuracea* (L) for elimination of Bezacryl Red GRL 180 from aqueous solution: equilibrium and kinetic studies

Laid Guemou^{a,b,*}, Samir Kadi^c, Salima Lellou^c, Badreddine Moussaoui^b, Nadjib Benzohra^b, Mohamed Sassi^{a,d}

^aLaboratory of Improvement and Valorization of Local Animal Productions, University of Tiaret BP 78 Zaaroura, Tiaret 14000, Algeria, email: Laidgue@gmail.com (L. Guemou)

^bLife and Natural Science Department, University Center of Tissemsilt, Route de BOUGARA, Ben Hamouda, 38004, Tissemsilt, Algeria, emails: moussmed@hotmail.fr (B. Moussaoui), nadjib-22@hotmail.com (N. Benzohra)

^cLaboratory of Plant Physiology Applied to Above-Soil Culture, University of Tiaret BP 78 Zaaroura, Tiaret 14000, Algeria, emails: ksam792002@yahoo.fr (S. Kadi), lellousalima@yahoo.fr (S. Lellou)

^dLife and Natural Sciences Faculty Ibn-Khaldoun University, Tiaret BP 78 Zaaroura, Tiaret 14000, Algeria, email: mo_sassi@yahoo.fr (M. Sassi)

Received 25 August 2020; Accepted 15 January 2021

ABSTRACT

In this study, biosorption of the dye Bezacryl Red GRL 180 by two fractions of the lichen *Pseudevernia furfuracea* L one greater than 250 μm and the other less than 250 μm , was investigated in batch system. Operating variables like biomass amount, pH, contact time, temperature, and dye concentration were explored. Fourier-transform infrared spectroscopy analyses delivered information about the possible binding groups present in the lichen, as aliphatic chains, carboxylic, and sulfonate groups. The results of batch kinetic experiments were well fitted by pseudo-second-order for the two materials. Equilibrium data were well described by the Freundlich isotherms for the two fractions of our lichen. Under optimized batch conditions, up to 121.95 mg g^{-1} for the lower fraction and 188.68 mg g^{-1} for the greater than 250 μm could be removed from solution in a relatively short time. These values show that our lichen by these two fractions has better adsorption efficiency for this industrial dye.

Keywords: Biosorption; Bezacryl Red GRL 180; *Pseudevernia furfuracea*; Kinetics; Equilibrium

1. Introduction

Since ancient times, individuals have been interested with colors. From cave canvases to the most recent contraptions, color has been a consistent companion of people [1]. Dyes are chemical substances basically used to impart color to objects [2], most dyes are complex organic molecules and they should be resistant to physical and chemical exposure. Synthetic dyes are used extensively in the majority of today's technological areas such as especially textile industry, leather tanning, paper manufacturing, food

industry, agricultural research, and cosmetics [3]. In recent times, contamination of water sources with this aesthetic poison as a consequence of various industrial activities has become a serious problem. Discharge of dye contaminated wastewaters into the aquatic environment without adequate treatment can lead to adverse effects on the aesthetic quality of water bodies and impact the ecosystem by reducing the sunlight penetration, which in turn disturbs the photosynthetic activities in the aquatic system; and occurrence of chronic and acute toxicity [4], and gas solubility in water. In addition, the textile dyes may be carcinogenic or mutagenic in nature and can produce toxic amine compounds

* Corresponding author.

under degradative conditions [5,6]. In conjunction with these hurtful properties most dyes are idle and non-biodegradable [7]. In this sense, special mention should be made to azo-type textile dyes which, around 15%–50%, do not bind to the fabric, during the dyeing process, and are released into wastewater, which is commonly used, in developing countries, for the purpose of irrigation in agriculture [8]. The use of these azo compounds is very negative to soil microbial communities [9] and to germination and growth of plants [8]. Therefore, the treatment of dye contaminated aquatic systems and the improvement of water quality are important topics in the field of environmental technologies.

Different techniques for the elimination of “emerging” pollutants such as ion exchange, electrolysis, precipitation, chemical oxidation, fluctuation and many others have been reported earlier [10]. In any case, long operational time, tall processing cost, plausible poisonous side items arrangement abridges their utilization on bigger scale [11]. Because synthetic dyes cannot be efficiently removed from the wastewaters by conventional methods, their adsorption on inexpensive and efficient solid supports is considered as a simple and economical method for their removal from wastewaters [12]. Biosorption is an alternative environmentally friendly technique to current costly water treatment technologies and based on the interaction between biomaterial and pollutant. It is one of the leading treatment strategies due to its flexibility, simplicity of design, and insensitivity to toxic pollutants [12]. Biosorption of different pollutants by various biological materials has been studied widely in the last years for its potential for wastewater treatment [13,14]. Different natural materials, such as blue-green algae [15], green macroalgae [16], brown marine algae [17] nonliving green algae [18], brown seaweeds [19], fungal biomass [20], bacteria [21,22], peat biomass [23], aquatic mosses [24], cellulose/chitin beads [25], tree fern [26], halloysite-based [27], modified kaolinite [28] and many other adsorbents have been applied to remove a lot of pollutants from solution.

Lichens are life forms comprising of a fungus and an alga or cyanobacterium which combine in a symbiotic relationship with a few one of kind physiological and morphological characteristics [29]. These organisms have many applications in medicine, food and environment. However lichens don't have a complex root system, waxy cuticle or stoma, and consequently they obtain most of their nutrients from the air and dry deposition [30]. That's why they have been broadly utilized as atmospheric pollution indicators since of their ability to emphatically tie and gather metals [31,32]. The metal-ion binding properties of lichens have been found that nonliving lichen biomass is able to bond metal-ions more than living lichens [31] since the living plasma layer excludes metals from entering the cell [33]. The component cation uptake by these organisms is generally regarded as an abiotic process governed by surface complexation of cations with different functional groups exposed on here surface [34]. These functional groups may be carboxylic, hydrocarboxylic acids and chitin heave [33]. Recently, several workers observed a high potential of lichen for the adsorption of many pollutants such as chromate anions [35], chromium and lead [36], mercury [37]. Removal of pollutants from water by biosorption, using lichen as a composite material and dead biomass can be a promising process.

In the present paper, biosorption of Bezacryl Red GRL 180 by the dead biomass of the lichen *Pseudevernia furfuracea* L has been investigated. This dye is highly water-soluble and can have a harmful effect on aquatic life with long-lasting effects [38]. The biosorption equilibrium and kinetic data are fitted using different models and process parameters were evaluated.

2. Materials and methods

2.1. Adsorbent

The lichen *Pseudevernia furfuracea* L used in this study was collected from the national park of Theniet El had in the province of Tissemsilt (Northern Algeria). It was washed to eliminate all impurities and then dried in an oven (Memmert) for 24 h at 80°C. Then ground and sieved by a 250-micrometer sieve to have two fractions less than 250 micrometers and greater than 250 micrometers with which we will work along with this study.

2.2. Characterization of materials

2.2.1. Morphological analysis

Morphological analysis by scanning electron microscopy (SEM) has been carried out to provide information on the state of the surface of our adsorbent.

2.2.2. Fourier-transform infrared spectroscopy

The identification of functional groups on the surface of our biosorbents was performed by infrared spectroscopy. The two fractions were analyzed by Fourier-transform infrared spectroscopy (FTIR) in solid form. Using a diffuse reflectance accessory, spectra were registered from 4,000 to 400 cm^{-1} .

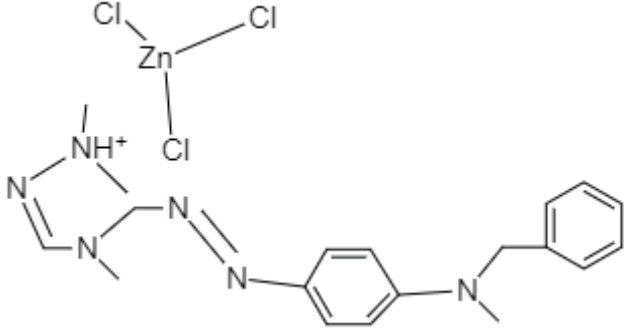
2.3. Adsorbate

The dye considered in this study is Bezacryl Red GRL 180, it was prepared from powder in the laboratory by dissolving it in distilled water. This powder was provided by the textile blanket manufacturing company “SOFACT” Tissemsilt (Northern Algeria). Its characteristics are summarized in Table 1.

2.4. Biosorption studies

Biosorption experiments were carried out in 200 mL Erlenmeyer flasks containing 100 mL of a solution of our dye red GRL 180 at a concentration of 25 mg L^{-1} and biomass of our material by stirring in a shaking water bath until we reach the adsorption equilibrium. After reaching equilibrium, the solutions were separated from the biomass by filtration through a colander followed by centrifugation (centrifuge 3K10) at a speed of 6000 revolutions per minute (rpm) for 5 min. The absorbance of the supernatant solution was measured by a UV-visible spectrophotometer (SHIMADZU UV-1202), at the wavelength which corresponds to the maximum absorbance of red GRL 180 ($\lambda_{\text{max}} = 525 \text{ nm}$) which was previously determined, and then

Table 1
Properties and characteristics of red GRL 180 [38]

Dye	Bezacryl Red GRL 180
Chemical name	5-[[4-[benzylmethylamino]phenyl]azo]-1,4-dimethyl-1H-1,2,4-triazolium trichlorozincate(1-)
Structure	
CAS number	38845-47-5
EC number	254-149-3
Molecular formula	C ₁₈ H ₂₃ Cl ₃ N ₆ Zn
Molecular weight (g mol ⁻¹)	495.16442
Content of zinc	3.7%
Specific wavelength (nm)	525 (this study)

the residual dye concentration is given by Beer–Lambert’s law, from a calibration curve. The biosorption capacity was determined by using the following equation:

$$Q_e = \frac{(C_i - C_e)V}{m} \quad (1)$$

where C_i and C_e represent the initial and equilibrium concentrations of dye red GRL 180 (mg L⁻¹), respectively V is the volume of the dye solution (L) and m is the amount of biosorbent (g).

2.5. Kinetic studies

The biosorption kinetics assumes an important role in the selection, design, and operation of adsorption systems. As previously elucidated, biosorption is a passive and metabolism-independent process [39]. The adsorption tests were carried out in a batch reactor, using a 1 L capacity glass, with stirring the synthetic solution of red GRL 180 in the presence of adsorbent “the two fractions of our lichen” at laboratory temperature. The homogenization of the mixtures was ensured by a magnetic bar stirrer with constant stirring at 200 rpm for 90 min. Samples were taken at regular time intervals and after separation of adsorbent adsorbate, using a colander and then centrifugation. The absorbance of the supernatant solution was measured with a UV spectrophotometer. The biosorption capacity was determined by using Eq. (1).

Batch biosorption kinetics of red GRL 180 uptake was examined by using the pseudo-first-order kinetic model of Lagergren, the pseudo-second-order kinetic model, and the intraparticle diffusion model. These equations are given as:

The Lagergren pseudo-first-order kinetic model [40]:

$$\ln(q_e - q_t) = \ln q_e - k_1 t \quad (2)$$

where q_e and q_t are the biosorption capacities of sorbent material at equilibrium, and time t (mg g⁻¹), respectively. k_1 is the rate constant for pseudo-first-order biosorption (min⁻¹).

The pseudo-second-order kinetic model [41]:

$$\frac{t}{q_t} = \frac{1}{k_2 q_2^2} + \frac{1}{q_2} t \quad (3)$$

with q_2 (mg g⁻¹) and k_2 (g mg⁻¹ min⁻¹) are the maximum biosorption capacity and the equilibrium rate constant for the pseudo-second-order biosorption, respectively.

The intraparticle diffusion model [42]:

$$q_t = k_p t^{1/2} + C \quad (4)$$

where C is the intercept and k_p is the intraparticle diffusion rate constant (mg g⁻¹ min^{-1/2}).

2.6. Isotherm studies

In equilibrium isotherm studies, the solution of red GRL 180 of different concentrations (10 to 200 mg L⁻¹) at optimal pH of the initial solution (pH = 9) was stirred with our materials in a shaker water bath at 30, 40 and 50°C for a contact period of 90 min. The equilibrium concentrations were determined by the absorbance of the solutions using a spectrophotometer after separation of the adsorbent and the adsorbate.

Batch flow biosorption applications were analyzed using adsorption isotherms models. Here Freundlich, Langmuir, Dubinin–Radushkevich (D–R), Elovich, Langmuir–Freundlich adsorption isotherm models were used to describe the equilibrium between the absorbed amount of red GRL 180 on both adsorbents and equilibrium concentration (C_e) of our dye in solution at a constant temperature.

Freundlich model assumes that the uptake of sorbate occurs on a heterogeneous surface of the sorbent. Langmuir model describes the monolayer sorption process onto the sorbent surface with specific binding sites. The linearized forms of the four models were used to compare between them.

The Freundlich equation is expressed as Eq. (5) [43]:

$$\ln q_e = \ln k + \left(\frac{1}{n}\right) \ln C_e \quad (5)$$

The Langmuir equation is expressed in Eq. (6) [44]:

$$\frac{C_e}{q_e} = \frac{1}{q_m k_L} + \frac{C_e}{q_m} \quad (6)$$

where k and n are Freundlich constants related to adsorption capacity and adsorption intensity, respectively. q_m and k_L the Langmuir equation represented the maximum adsorption capacity of adsorbents (mg g^{-1}) and Langmuir adsorption constant related to the free energy of adsorption.

The D–R isotherm is an empirical adsorption model that is generally applied to express the adsorption mechanism with Gaussian energy distribution onto heterogeneous surfaces. It presumes a multilayer character involving van der Waal's forces, applicable for physical adsorption processes [45].

D–R isotherm is expressed as follows [46]:

$$\ln q_e = \ln q_m - \beta \varepsilon^2 \quad (7)$$

$$\varepsilon = RT \ln \left(1 + \frac{1}{C_e}\right) \quad (8)$$

where ε is Polanyi potential, β is Dubinin–Radushkevich constant, R is gas constant ($0.008314 \text{ kJ mol}^{-1}\text{K}^{-1}$), T is the absolute temperature.

Elovich implies to multilayer adsorption by assuming that the adsorption sites increase exponentially with adsorption [47].

The linear equation of the Elovich model is expressed as follows [48]:

$$\ln \left(\frac{q_e}{C_e}\right) = \ln k_E q_m - \frac{q_e}{q_m} \quad (9)$$

where k_E is the Elovich equilibrium constant (L mg^{-1}), and q_m is the Elovich maximum adsorption capacity (mg g^{-1}).

The Redlich–Peterson isotherm is a mix of the Langmuir and Freundlich isotherms. This model is an empirical isotherm incorporating three parameters. The mechanism of

adsorption is a mix and does not follow ideal monolayer adsorption [49].

This model is defined by the following expression:

$$q_e = \frac{K_{RP} C_e M}{1 + (K_{RP} C_e)^\beta} \quad (10)$$

where K_{RP} is the equilibrium constant ($\text{d.m.}^3 \text{ mg}^{-1}$), β is the heterogeneity factor that depends on surface properties of the adsorbent, and M is the maximum amount adsorbed (mg g^{-1}).

2.7. Thermodynamic studies

The thermodynamic study is another vital consideration to explain the mechanism of adsorption through the energy and to determine what process will take place spontaneously. Thermodynamic parameters, such as enthalpy change (ΔH°), Gibb's free energy (ΔG°), and entropy change (ΔS°), were calculated using Van't Hoff Eq. (11):

$$\ln K_D = \frac{\Delta G^\circ}{T} = \frac{\Delta S^\circ}{R} - \frac{\Delta H^\circ}{RT} \quad (11)$$

where ΔH° is the change in enthalpy (J mol^{-1}), ΔS° is the entropy change ($\text{J mol}^{-1} \text{ k}^{-1}$), T is the absolute temperature (K). R is the universal gas constant ($8.314 \text{ J mol}^{-1} \text{ k}^{-1}$), and K_D is the distribution coefficient obtained by:

$$K_D = \frac{q_e}{C_e} \quad (12)$$

The values of ΔH° and ΔS° parameters can be evaluated from the gradient and intercept of the linear Van't Hoff plot of $\ln K_D$ against $1/T$ from Eq. (11).

3. Results and discussion

3.1. Characterizations of biosorbent

3.1.1. Morphological analysis

Observations with a scanning electron microscope, made on the two fractions of our lichen Fig. 1, show the presence of small grain aggregates for the fraction less than $250 \mu\text{m}$ and a long filamentous structure for the fraction greater than $250 \mu\text{m}$. Know that the lichen is a form of symbiosis between algae and fungi and given the colors of the two fractions (green for the lower fraction and white for the upper fraction) we can assume that these aspects (filamentous and granular) are linked to the nature of each fraction (fraction less than $250 \mu\text{m}$ is mainly made of algae and fraction greater than $250 \mu\text{m}$ is mainly consists of mycelium of fungi).

3.1.2. FTIR analysis

To better understand and confirm the nature of active sites on both biosorbents surfaces, the materials were analyzed by FTIR spectrometry. The spectrum of different fractions of our lichen is shown in Fig. 2. The two biosorbents

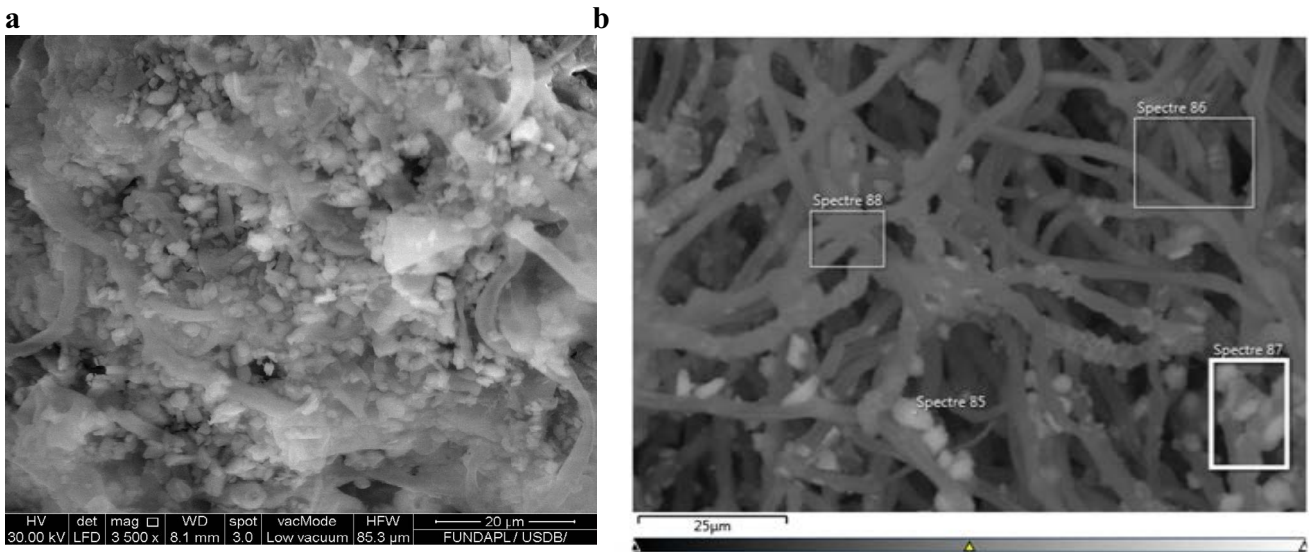


Fig. 1. Microscopic observation of the SEM of the two fractions (a) less than 250 μm and (b) greater than 250 μm .

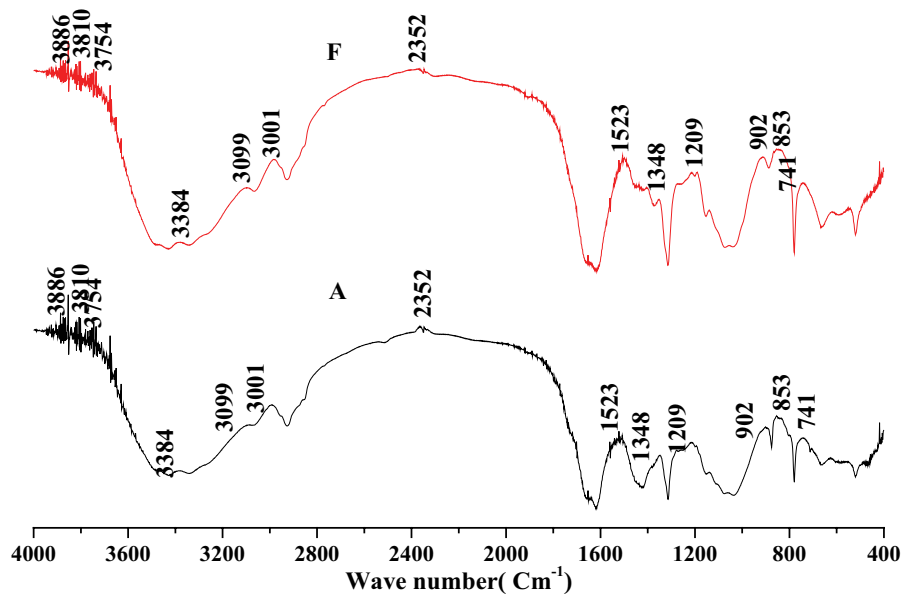


Fig. 2. FTIR spectra of different fractions of our lichen (A) fraction $<250 \mu\text{m}$ and (F) fraction $>250 \mu\text{m}$.

presents a similar biomass structure. The peaks at 3,886; 3,810; 3,754 and 3,384 cm^{-1} were attributed to hydroxyl stretch [50,51]. The peak at 3,099 cm^{-1} may be explained by symmetric and asymmetric stretches of aliphatic chains [51]. The large absorption band at 2,352 cm^{-1} represents the (–CH) groups [50] and C=O stretch of the carboxylic groups present in cell wall of the biomass like cellulose. The peaks at 1,523 cm^{-1} representing amid groups (–NH) [52]. The spectrum also shows peaks at 1,209 and 853 cm^{-1} should be due to the presence of S=O bending and C–S–O stretching vibrations, from ester sulfonate groups [53]. Other peaks can be observed at around 902 and 741 cm^{-1} could be assigned to, respectively, the aromatic C–H and bend methylene (CH_2) sacking [51].

3.2. Adsorption studies

3.2.1. Optimization of adsorption conditions

This manipulation aims to optimize the mass necessary “the solid/liquid ratio” (S/L ratio) as well as the optimal pH to have effective adsorption of GRL 180 red on the two fractions of our lichen. The results obtained are shown in Figs. 3 and 4.

As can be seen from Fig. 2 the biosorption capacity (q_e) was significantly decreased with increasing biomass amount a higher biosorption capacity obtained with a small amount of biosorbent (ratio of 0.5). The decreasing biosorption capacity with increasing biosorbent dosage may be explained that the adsorbent dosage is one of the

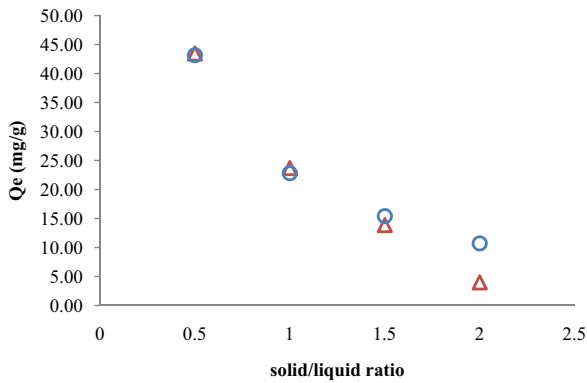


Fig. 3. Influence of the (S/L) ratio on the absorption of red GRL 180 by both biosorbents: (A) fraction <250 μm and (F) fraction >250 μm.

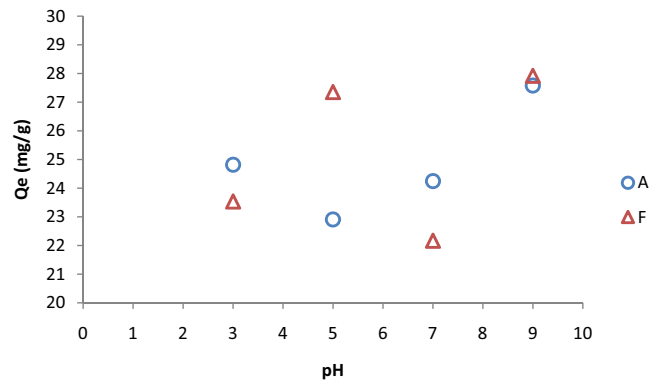


Fig. 4. Effect of pH on the absorption of red GRL 180 by the two fractions of our biosorbent: (A) fraction <250 μm and (F) fraction >250 μm.

crucial parameters when used in the determination of the adsorption capacity as per Eq. (1) above. Adsorbent dosage is the denominator; the lesser the amount of the adsorbents, the better efficiency of the adsorbent [54]. Meanwhile, the decrease in q_e with an increase in adsorbent dosages might be caused by particle interactions, such as aggregation caused by the high adsorbent concentration, which leads to a decrease in the surface area and saturation of solid particles.

Solution pH is a very important factor for the dye biosorption performance of a biomaterial and affects not only the surface charge of the biosorbent but also the dye chemistry in aqueous medium [55]. The reactive dye biosorption performance of both biosorbents was tested over the pH range from 3.0 to 9.0 (Fig. 3). We can see that the biosorption capacity of both biosorbents generally increases with increasing pH level. The higher adsorption capacity observed at basic pH (9.0) can be explained by the electrostatic attractive forces between dye cations and negatively charged biosorbent surface.

To better illustrate these results, we proceeded to the determination of the point of zero charge (pH_{ZPC}) which corresponds to the pH value for which the net charge of the adsorbent surface is zero. The results are presented in Fig. 5. As can be seen the pH_{ZPC} for the utilized biosorbents are (pH_{ZPC} = 4.8) for the fraction greater than 250 μm (F) and (pH_{ZPC} = 4.9) for the fraction less than 250 μm (A), which means that the adsorbent surface is positively charged at the pH less than pH_{ZPC} and negatively at a pH greater than pH_{ZPC}. The more the pH increases towards pH_{ZPC}, the more negative ion density on the surface of both biosorbents increases in turn, allowing more adsorption of red GRL 180 cations.

3.2.2. Biosorption kinetics

The evolution of the adsorbed amount of red GRL 180 as a function of time is illustrated in Fig. 6. The kinetics of adsorption of the dye on the materials used has almost the same appearance, characterized by strong adsorption of the dye from the first minutes of contact, followed by a slow increase until reaching a state of equilibrium.

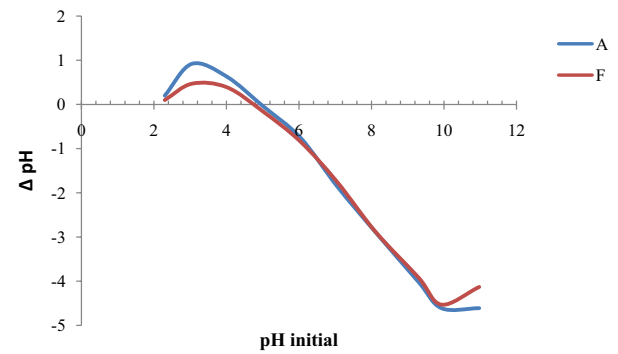


Fig. 5. The points of zero charge for the utilized biosorbents.

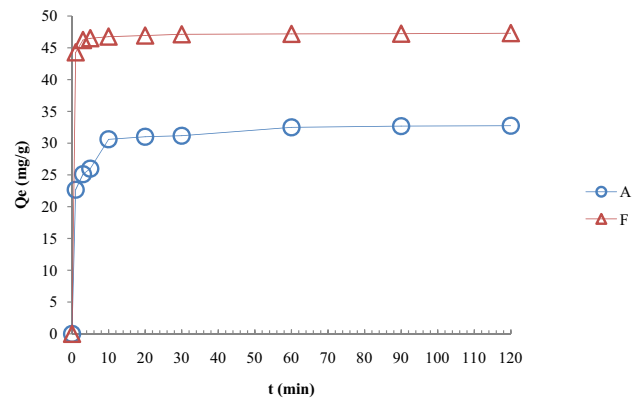


Fig. 6. Effect of the contact time on the fixation of the red GRL 180 on the two fractions. Conditions: V = 100 mL; C = 25 mg L⁻¹; S-L ratio = 0.5; T = 25°C; pH = 9 (A) fraction <250 μm and (F) fraction >250 μm.

The kinetics of rapid adsorption during the first minutes of reaction (10 min), can be interpreted by the fact that at the start of adsorption, the number of active sites available on the surface of the adsorbent material is much greater than the sites remaining after a while [56]. Thus it can be noted that the quantity adsorbed by the fraction greater than 250 μm is greater than that adsorbed by the fraction less than 250 μm this may be due to the nature of the material

(the fraction less than 250 μm which is mainly constituted of algae whereas the second fraction consists mainly of mycelium of fungi).

The application of mathematical models of kinetics (pseudo-first-order, pseudo-second-order and intraparticle diffusion model) on our results allowed the prediction of the adsorption mechanism of red GRL 180 on the different materials used. The linearization parameters determined from the curves of the two models are summarized in Table 2. All parameters and values of Figs. 7 and 8 are summarized in Table 2.

The results show that the adsorption of red GRL 180 follows the pseudo-second-order model perfectly with correlation coefficients, R^2 of more than 0.99, the average relative error (ARE %) low compared to the results of the pseudo-first-order model, and the maximum adsorption capacities q_e calculated from the pseudo-second-order model are in accordance with the experimental values for the two biosorbents. This model suggests that adsorption depends on the adsorbate-adsorbent pair. It is also physisorption although the contribution of chemisorption is not to be ruled out.

Fitting the data to the intraparticle diffusion model indicated the intraparticle diffusion was not only a rate-controlling step (the plots did not go through the origin $C > 0$) and hence it can be suggested that the external mass transfer and intraparticle diffusion were collectively controlled the adsorption process.

3.2.3. Isotherms studies

Isotherm studies are important applications for the understanding of the biosorption mechanism. The adsorption isotherms of red GRL 180 at 20°C, 40°C and 50°C by both biosorbents are shown in Fig. 9. According to the classification of Giles et al. [57], the adsorption isotherms of red GRL 180 are L for both materials and whatever the temperature.

In the temperature range considered, the isotherms of the tow fraction less than 250 μm and greater than 250 μm

show an increase in the quantity adsorbed as the temperature increases, which means that the process involved is endothermic.

The adsorption isotherms give a lot of fundamental physicochemical data to estimate the applicability of the adsorption process, express the surface properties of the adsorbent, and can also be used to find the maximum adsorption capacity of a mass [58]. The last step in the study of isotherms consists in modeling the curve, or more precisely, in accounting by a mathematical equation for the whole of the curve. The Freundlich and Langmuir models are the most frequently used models for describing experimental adsorption isotherm data, due to their simplicity.

The parameters obtained from the modeling of the experimental results of the sorption isotherms of red GRL 180 by the two fractions are summarized in Table 3.

Based on the correlation coefficients, as well as the mean relative errors (ARE %) presented in the Table 3 and Figs. 10–12, we can say that, for the two-parameter isotherm category, the Freundlich model is higher than the Langmuir model. This showed that the Freundlich model better describes the adsorption isotherms of red GRL 180 on the two fractions less than and greater than 250 μm . However, Freundlich's isotherm model assumes heterogeneity of the adsorption surface with sites of different adsorption energies, as well as the possibility of multilayer formation of the adsorbed molecules with interactions between them [42]. In this study, all the values of n are positive, which shows that this type of adsorption is favorable.

The Elovich isotherm constants, k_E and q_m , as well as the coefficient of correlation, R^2 , for the red GRL 180 adsorption process using the two fractions are obtained using the linear form of the equation (Table 3). In all cases, the Elovich isotherm exhibited lower coefficients of correlation (between 0.41 and 0.79). Therefore, the Elovich model is unable to describe the adsorption isotherms of red GRL 180 onto both biosorbents. On the other hand, and despite the lower correlation coefficients, the values of maximum adsorption capacity determined using the linear transformation of

Table 2
Kinetic parameters red GRL 180 adsorption onto both adsorbents

Kinetic model	Parameters	Adsorbents	
		Fraction <250 μm	Fraction >250 μm
Pseudo-first-order	$Q_{e,\text{exp}}$ (mg g^{-1})	32.74	47.29
	$Q_{e,\text{cal}}$ (mg g^{-1})	7.24	1.03
	k_1 (min^{-1})	-0.055	-0.033
	R^2	0.96	0.76
	ARE %	83.62	99.08
Pseudo-second-order	$Q_{e,\text{exp}}$ (mg g^{-1})	32.74	47.29
	$Q_{e,\text{cal}}$ (mg g^{-1})	33.00	47.39
	k_2 (g mg min^{-1})	0.028	0.19
	R^2	0.99	1
	ARE %	4.78	1.12
Intraparticle diffusion model	k_p ($\text{mg g}^{-1} \text{min}^{-1/2}$)	0.41	0.22
	C	29.17	45.94
	R^2	0.95	0.94

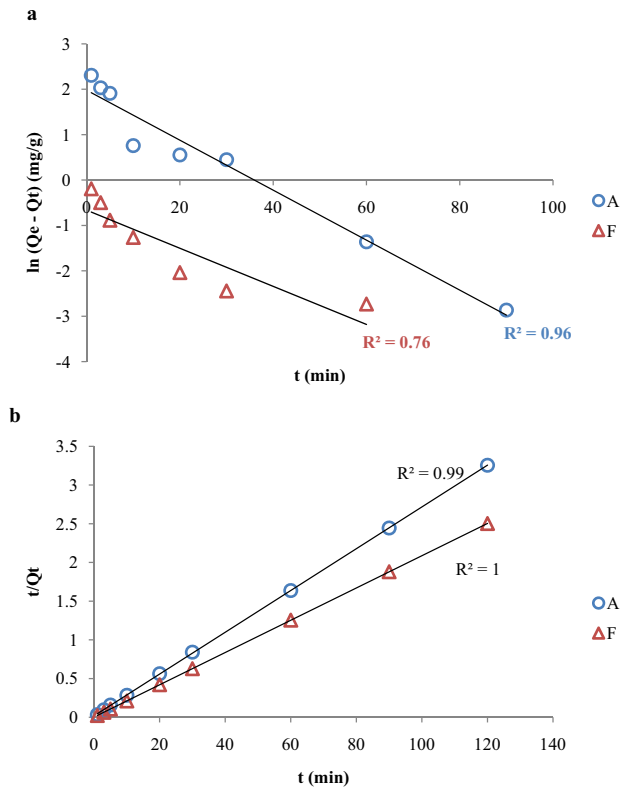


Fig. 7. Kinetic models for the adsorption of red GRL 180 onto both biosorbents (a) pseudo-first-order and (b) pseudo-second-order.

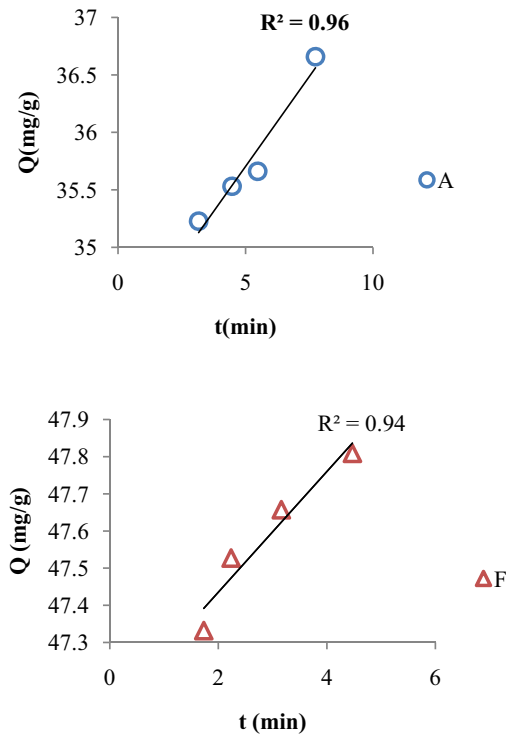


Fig. 8. Kinetic intraparticle model for the adsorption of red GRL 180 onto both biosorbents.

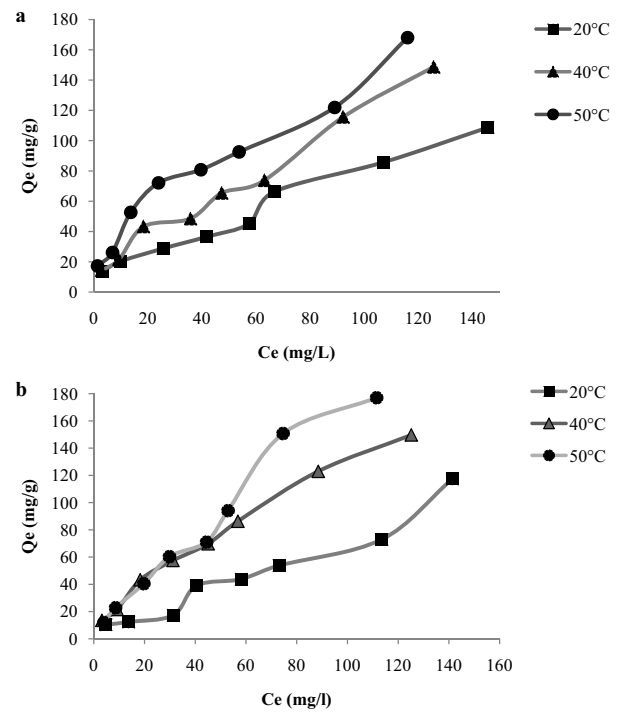


Fig. 9. Isothermal adsorption of GRL red at 20°C, 40°C and 50°C by the two fractions (a) less than 250 μm and (b) greater than 250 μm of our biosorbents.

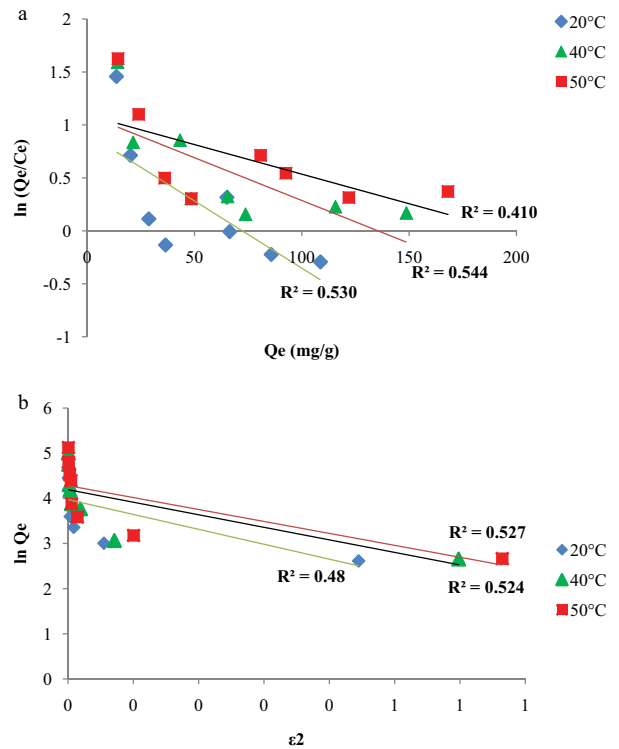


Fig. 10. Isotherms model of (a) Elovich and (b) D-R for red GRL 180 adsorptions onto fraction <250 μm .

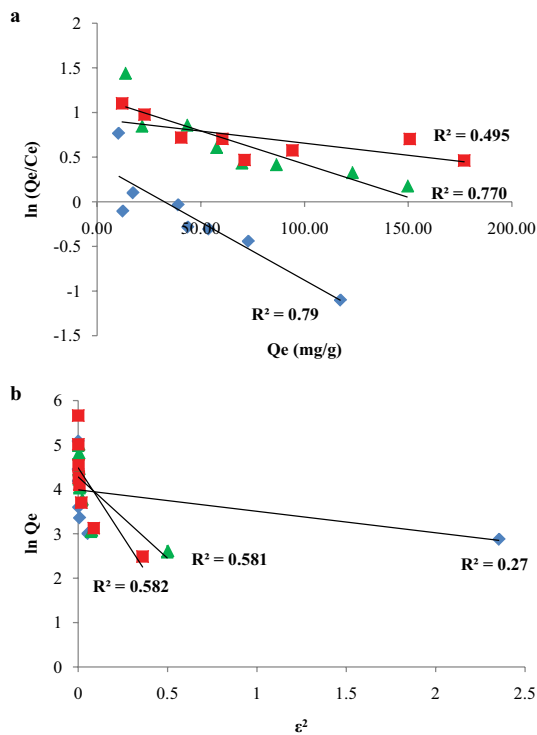


Fig. 11. Isotherms model of (a) Elovich and (b) D–R for red GRL 180 adsorptions onto fraction $>250 \mu\text{m}$.

the Elovich equation (Table 3) are very close to the experimental adsorbed quantities at equilibrium. This means that the hypothesis of exponential coverage of adsorption sites which involves multilayer adsorption agrees with experience in the concentration range studied.

The sorption data were applied to the D–R model to distinguish between physical and chemical adsorption. The magnitude of all parameters (q_m , β , E) is useful for information about the type of adsorption processes, such as chemical or physical adsorption. All values of the parameters are given in Table 3. It can be seen that the E values varied from 0.28–1.02 kJ mol^{-1} at all temperatures, indicating that the adsorption of red GRL 180 may be interpreted as physical adsorption.

The three-parameter models have also been applied to evaluate the fit by isotherm for the adsorption of a lot of pollutants. The calculated isotherm parameters for the Redlich–Peterson model and their corresponding correlation coefficients, R^2 , values are shown in Table 3. Redlich–Peterson's model describes very well our adsorption isotherms given the high values of R^2 ($R^2 > 0.96$) and the low values of the average relative error which does not exceed 22.22%. The K_{RP} values showed that the adsorption capacity increased with increasing temperature for the fraction less than $250 \mu\text{m}$, similar behavior has also been observed with experimental isotherms. The surface heterogeneity factor, β , depends on the surface properties like the distribution of the active sites. The value of this parameter is <1 for all fractions. This result is a sign of favorable adsorption.

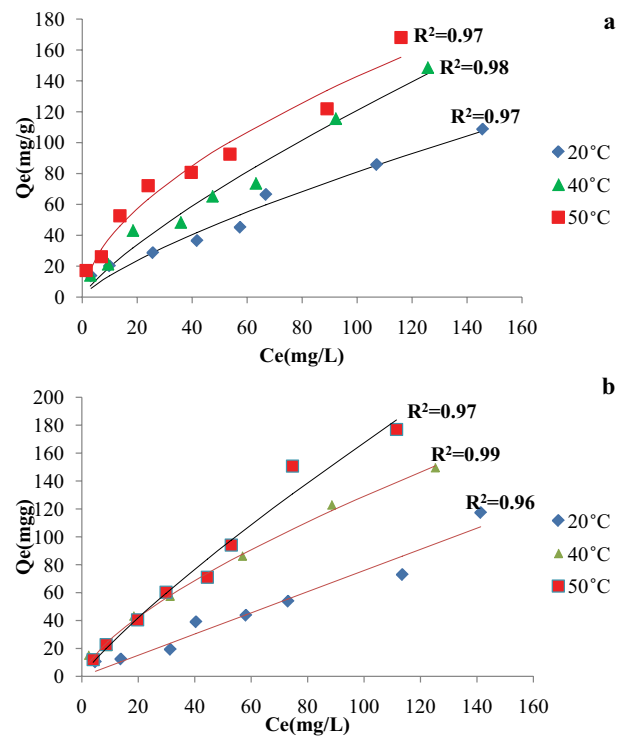


Fig. 12. Isotherms model of Redlich–Peterson for red GRL 180 adsorption onto fraction $<250 \mu\text{m}$ (A) and fraction $>250 \mu\text{m}$ (F).

3.2.4. Thermodynamic parameters

The parameters such as free energy, ΔG° , enthalpy ΔH° , and entropy ΔS° for adsorption of red GRL 180 onto our biosorbents are listed in Table 4.

In the case of physisorption, the variation of the free energy is between 0 and 20 kJ mol^{-1} [59], as for the chemisorption it is in the range 80–400 kJ mol^{-1} [60]. The positive ΔG° values at 20°C ($\Delta G^\circ < 20 \text{ kJ mol}^{-1}$) mean that the physisorption is not a spontaneous process but the negative ΔG° values at the other temperature mean that it is a spontaneous process. $\Delta S^\circ > 0$ confirms the disorder of the process and suggest that some structural changes in the biosorbent surface. The positive ΔH° values mean that the process is endothermic. This observation confirmed the trend of the q_m values obtained from the Langmuir isotherm model with different temperatures.

4. Conclusions

The absorption of an industrial dye red GRL 180 by the dead biomass of the lichen *Pseudevernia furfuracea* L can be considered as an innovative and promising process with good performance. Experiments have shown that the adsorption equilibrium of red GRL 180 by our materials is estimated at 60 min, but it is rapid during the first minutes of reaction (10 min). The biosorption kinetics of red GRL 180 is rapid and perfectly follows the pseudo-second-order model. The latter suggests that adsorption depends on the adsorbate-adsorbent pair. The intraparticle diffusion model

Table 3
Parameters of equilibrium models for red GRL 180 biosorption onto the lichen *Pseudevernia furfuracea* L

Isotherms models	Parameters	Absorbents					
		Fraction <250 μm			Fraction >250 μm		
		20°C	40°C	50°C	20°C	40°C	50°C
Freundlich	K_F	6.00	6.38	9.00	3.41	5.64	3.11
	n	1.79	1.62	1.54	1.57	1.48	1.23
	R^2	0.93	0.96	0.96	0.92	0.99	0.98
	ARE %	15.48	13.10	14.26	22.02	5.79	17.68
	$Q_{e,\text{exp}}$ (mg g^{-1})	108.69	148.72	168.09	117.37	149.67	177.01
Langmuir	q_m (mg g^{-1})	60.61	81.97	121.95	59.52	104.17	188.68
	k_L (mg^{-1})	0.08	0.067	0.065	0.05	0.04	0.02
	R^2	0.85	0.89	0.95	0.76	0.93	0.99
	ARE %	31.10	22.72	25.49	26.68	18.06	13.19
	q_m (mg g^{-1})	78.74	143.26	178.57	76.92	135.14	370.37
Elovich	k_E	0.032	0.024	0.017	0.02	0.024	0.007
	R^2	0.53	0.54	0.41	0.79	0.77	0.49
	ARE %	30.09	26.18	41.85	15.35	30.33	48.71
	q_m (mg g^{-1})	53.19	66.22	72.40	54	72.16	88.76
	β	3.3×10^{-6}	2.8×10^{-6}	2.7×10^{-6}	5×10^{-6}	3.7×10^{-6}	6.2×10^{-6}
D-R	E (kJ mol^{-1})	0.389	0.424	0.43	1.02	0.36	0.28
	R^2	0.48	0.52	0.52	0.27	0.58	0.58
	ARE %	47.77	44.33	52	54.54	52.99	45.16
	M (mg g^{-1})	0.489	0.649	0.930	120.710	30.868	185.102
	β	0.278	0.253	0.443	$3.19 \cdot E^{-11}$	0.380	0.289
Redlich–Peterson	K_{RP}	14.152	13.507	86.26	0.013	0.155	0.018
	R^2	0.97	0.98	0.98	0.96	0.99	0.97
	ARE %	19.18	17.60	14.92	22.22	11.50	16.10

Table 4
Thermodynamic parameters

Biosorbents	ΔH° (kJ mol^{-1})	ΔS° (kJ mol^{-1})	ΔG° (kJ mol^{-1})			R^2
			293	313	323	
Fraction <250 μm	27.11	0.090	0.69	-1.10	-2.01	0.89
Fraction >250 μm	29.947	0.098	1.085	-0.884	-1.869	0.99

show that the external mass transfer and intraparticle diffusion were collectively controlled the adsorption process. The equilibrium is well described by the Freundlich model on the two fractions less and greater than 250 μm . The thermodynamic parameters data show that the adsorption was not spontaneous endothermic disordered at 20°C and it became spontaneous endothermic ordered at 40° and 50°C. By its quantities adsorbed at equilibrium ($Q_e = 121 \text{ mg g}^{-1}$ for the fraction less than 250 and ($Q_e = 188 \text{ mg g}^{-1}$ for the fraction greater than 250) we can say that our biosorbents are better than several biosorbents (aquatic mousses, tree fern, and marine algae) and constitute promoter materials.

Acknowledgments

This work is also partially supported by the research laboratory of Improvement and Valorization of Local Animal

Productions, University of Tiaret, under the aegis of the General Direction of research and development technologies/Ministry of Higher Education and Research Sciences DGRSDT/MERS (Algeria).

References

- [1] J. Mittal, Permissible synthetic food dyes in India, *Resonance – J. Sci. Educ.*, 25 (2020) 567–577.
- [2] T. Robinson, G. McMullan, R. Marchant, P. Nigam, Remediation of dyes in textile effluent: a critical review on current treatment technologies with a proposed alternative, *Bioresour. Technol.*, 77 (2001) 247–255.
- [3] T.V. Ramachandra, N. Ahalya, R.D. Kanamadi, Biosorption: Techniques and Mechanisms, CES Technical Report 110, Centre for Ecological Sciences, Indian Institute of Science, Bangalore, 2005.
- [4] M. Arami, N.Y. Limaee, N.M. Mahmoodi, N.S. Tabrizi, Equilibrium and kinetics studies for the adsorption of direct

- and acid dyes from aqueous solution by soy meal hull, J. Hazard. Mater., 135 (2006) 171–176.
- [5] C.I. Pearce, J.R. Lloyd, J.T. Guthrie, The removal of color from textile wastewater using whole bacterial cells: a review, Dyes Pigm., 58 (2003) 179–196.
- [6] M. Shin, T. Nguyen, J. Ramsay, Evaluation of support materials for the surface immobilization and decoloration of amaranth by *Trametes Versicolor*, Appl. Microbiol. Biotechnol., 60 (2002) 218–223.
- [7] C. Arora, S. Soni, S. Sahu, J. Mittal, P. Kumar, P.K. Bajpai, Iron based metal organic framework for efficient removal of methylene blue dye from industrial waste, J. Mol. Liq., 284 (2019) 343–352.
- [8] K. Rehman, T. Shahzad, A. Sahar, S. Hussain, F. Mahmood, M.H. Siddique, M.A. Siddique, M.I. Rashid, Effect of Reactive Black 5 azo dye on soil processes related to C and N cycling, PeerJ, 6 (2018) e4802, doi: 10.7717/peerj.4802.
- [9] N.R. Rane, V.V. Chandanshive, A.D. Watharkar, R.V. Khandare, T.S. Patil, P.K. Pawar, Phytoremediation of sulfonated Remazol Red dye and textile effluents by *Alternanthera philoxeroides*: an anatomical, enzymatic and pilot scale study, Water Res., 83 (2015) 271–281.
- [10] D. Pan, S. Ge, J. Zhao, J. Tian, Q. Shao, L. Guo, X. Mai, T. Wu, V. Murugadoss, H. Liu, T. Ding, S. Angaiah, Z. Guo, Synthesis and characterization of ZnNiIn layered double hydroxides derived mixed metal oxides with highly efficient photoelectrocatalytic activities, Ind. Eng. Chem. Res., 58 (2019) 836–848.
- [11] V. Kumar, P. Saharan, A.K. Sharma, A. Umar, I. Kaushal, A. Mittal, Y. Al-Hadeethi, B. Rashad, Silver doped manganese oxide-carbon nanotube nanocomposite for enhanced dye-sequestration: isotherm studies and RSM modelling approach, Ceram. Int., 46 (2020) 10309–10319.
- [12] S.K. Sharma, Green Chemistry for Dyes Removal from Wastewater: Research Trends and Applications, Wiley and Scrivener Publishing, New Jersey, 2015.
- [13] B. Volesky, Sorption and Biosorption, BV Sorbex, Quebec, 2003.
- [14] B. Volesky, Z.R. Holan, Biosorption of heavy metals, Biotechnol. Progr., 11 (1995) 235–250.
- [15] K. Chojnacka, A. Chojnacki, H. Górecka, Biosorption of Cr^{3+} , Cd^{2+} and Cu^{2+} ions by blue-green algae *Spirulina* sp.: kinetics, equilibrium and the mechanism of the process, Chemosphere, 59 (2005) 75–84.
- [16] W.-Y. Lee, W.X. Wang, Metal accumulation in the green macroalga *Ulva fasciata*: effects of nitrate, ammonium, and phosphate, Sci. Total Environ., 278 (2001) 11–22.
- [17] Z.R. Holan, B. Volesky, Biosorption of Cd by biomass of marine algae, Biotechnol. Bioeng., 41 (1993) 819–825.
- [18] E. Fourest, B. Volesky, Alginate properties and heavy metal biosorption by marine algae, Appl. Biochem. Biotechnol., 67 (1997) 33–44.
- [19] M.M. Figueira, B. Volesky, V.S.T. Ciminelli, F.A. Roddick, Biosorption of metals in brown seaweed biomass, Water Res., 34 (2000) 196–204.
- [20] A. Kapoor, R. Viraraghavan, Removal of heavy metals from aqueous solutions using immobilized fungal biomass in continuous mode, Water Res., 32 (1998) 1968–1977.
- [21] P.G. Wightman, J.B. Fein, Ternary interactions in a humic acid-Cd-bacteria system, Chem. Geol., 180 (2001) 55–65.
- [22] N. Rangsayatorn, E.S. Upatham, M. Kruatrachue, P. Pothititayook, G.R. Lanza, Phytoremediation potential of *Spirulina* (*arthrospira*) *platensis*: biosorption and toxicity studies of cadmium, Environ. Pollut., 119 (2002) 45–53.
- [23] W. Ma, J.M. Tobin, Development of multimetal binding model and application to binary metal biosorption onto peat biomass, Water Res., 37 (2003) 3967–3977.
- [24] R.J.E. Martins, R. Pardo, R.A.R. Boaventura, Cadmium(II) and zinc(II) adsorption by the aquatic moss *Fontinalis antipyretica*: effect of temperature, pH and water hardness, Water Res., 38 (2004) 693–699.
- [25] D. Zhou, L. Zhang, J. Zhou, S. Guo, Cellulose/chitin beads for adsorption of heavy metals in aqueous solution, Water Res., 38 (2004) 2643–2650.
- [26] Y.S. Ho, C.C. Wang, Pseudo-isotherms for the sorption of cadmium ion onto tree fern, Process. Biochem., 39 (2003) 1–5.
- [27] I. Anastopoulos, A. Mittal, M. Usman, J. Mittal, G. Yu, A. Nunez-Delago, M. Kornaros, A review on halloysite-based adsorbents to remove pollutants in water and wastewater, J. Mol. Liq., 269 (2018) 855–868.
- [28] S. Lellou, S. Kadi, L. Guemou, J. Schott, H. Benhebal, study of methylene blue adsorption by modified kaolinite by dimethyl sulfoxide, Ecol. Chem. Eng. S, 27 (2020) 225–239.
- [29] A. Ates, A. Yildiz, N. Yildiz, A. Calimli, Heavy metal removal from aqueous solution by *Pseudevernia furfuracea* (L.) Zopf, Anal. Chim., 97 (2007) 385–393.
- [30] R.N. Williams, R.C. Casellas, N.F. Mangelson, L.B. Rees, L.L. Clair, G.B. Schaalje, K.D. Swalberg, Elemental analysis of lichens from the intermountain Western USA using PIXE, Nucl. Instrum. Methods Phys. Res., Sect. B, 109/110 (1996) 336–340.
- [31] G. Akcin, O. Salyabas, F. Yesilcimen, Biosorption of heavy metal from aqueous solution by dried lichens, Int. J. Chem., 11 (2001) 141–146.
- [32] O.W. Purvis, B.J. Williamson, K. Bartok, N. Zoltani, Bioaccumulation of lead by the lichen *Acarospora smaragdula* from smelter emissions, Res. New Phytol., 147 (2000) 591–599.
- [33] M.K. Chettri, C.M. Cook, E. Vardaka, T. Sawidis, T. Lanaras, The effect of Cu, Zn and Pb on the chlorophyll content of the lichens *Cladonia convoluta* and *Cladonia rangiformis*, Environ. Exp. Bot., 39 (1998) 1–10.
- [34] M. Pipiska, M. Hornik, L. Vrtoch, J. Augustin, J. Lesny, Biosorption of Co^{2+} ions by lichen *Hypogymnia physodes* from aqueous solutions, Biologia, 62 (2007) 276–282.
- [35] A. Bingol, A. Aslanb, A. Kackia, Biosorption of chromate anions from aqueous solution by a cationic surfactant-modified lichen (*Cladonia rangiformis* (L.)), J. Hazard. Mater., 161 (2009) 747–752.
- [36] O.D. Uluzozlu, A. Sari, M. Tuzen, M. Soylak, Biosorption of Pb(II) and Cr(III) from aqueous solution by lichen (*Parmelina tiliaceae*) biomass, Bioresour. Technol., 99 (2008) 2972–2980.
- [37] M. Tuzen, A. Sari, D. Mendil, M. Soylak, Biosorptive removal of mercury(II) from aqueous solution using lichen (*Xanthoparmelia conspersa*) biomass: kinetic and equilibrium studies, J. Hazard. Mater., 169 (2009) 263–270.
- [38] CHT Group, Bezacryl Golden Yellow GRL 180, Unpublished Internal Company Document, 2017.
- [39] S.C.R. Santos, G. Ungureanu, I. Volf, R.A.R. Boaventura, C.M.S. Botelho, In: V. Popa, Ed., Biomass as Renewable Raw Material to Obtain Bioproducts of High-Tech Value, Elsevier, Amsterdam, 2018, pp. 69–112.
- [40] S. Lagergren, Zur Theorie der Sogenannten Adsorption Gelöster Stoffe, Kungliga Svenska Vetenskapsakademiens, Handlingar, 24 (1898) 1–39.
- [41] Y.S. Ho, G. McKay, Kinetic models for the sorption of dye from aqueous solution by wood, Process Saf. Environ. Prot., 76 (1998) 183–191.
- [42] W.J. Weber, J.C. Morris, Kinetics of adsorption on carbon from solution, Sanitary Eng. Div., 89 (1963) 31–39.
- [43] H.M.F. Freundlich, Over the adsorption in solution, J. Phys. Chem., 57 (1906) 385–471.
- [44] I. Langmuir, The adsorption of gases on plane surfaces of glass, mica and platinum, J. Am. Chem. Soc., 40 (1918) 1361–1403.
- [45] O. Çelebi, C. Üzümlü, T. Shahwan, H.N. Erten, A radiotracer study of the adsorption behavior of aqueous Ba^{2+} ions on nanoparticles of zero-valent iron, J. Hazard. Mater., 148 (2007) 761–767.
- [46] N. Ayawei, A.T. Ekubo, D. Wankasi, E.D. Dikio, Adsorption of congo red by $\text{Ni}/\text{Al}-\text{CO}_3$: equilibrium, thermodynamic and kinetic studies, Orient. J. Chem., 31 (2015) 1307–1318.
- [47] M. Gubernak, W. Zapała, K. Kaczmarek, Analysis of amylbenzene adsorption equilibria on an RP-18e chromatographic column, Acta Chromatogr., 13 (2003) 38–59.
- [48] P.S. Kumar, S. Ramalingam, S.D. Kirupha, A. Murugesan, S. Vidhyadevi, S. Sivanesan, Adsorption behavior of nickel(II) onto cashew nutshell: equilibrium, thermodynamics, kinetics, mechanism and process design, Chem. Eng. J., 1169 (2010) 122–131.

- [49] F. Brouers, T.J. Al-Musawi, On the optimal use of isotherm models for the characterization of biosorption of lead onto algae, *J. Mol. Liq.*, 212 (2015) 46–51.
- [50] P.X. Sheng, Y.P. Ting, J.P. Chen, L. Hong, Sorption of lead, copper, cadmium, zinc, and nickel by marine algal biomass: characterization of biosorptive capacity and investigation of mechanisms, *J. Colloid Interface Sci.*, 275 (2004) 131–141.
- [51] J. Coates, Interpretation of Infrared Spectra, A Practical Approach, In: Encyclopedia of Analytical Chemistry, John Wiley & Sons Ltd., Chichester, 2000, pp. 10815–10837.
- [52] V. Murphy, H. Hughes, P. McLoughlin, Cu(II) binding by dried biomass of red, green and brown macroalgae, *Water Res.*, 41 (2007) 731–740.
- [53] E. Murano, R. Toffanin, E. Cecere, R. Rizzo, S.H. Knutsen, Investigation of the carrageenans extracted from *Solieria filiformis* and *Agardhiella subulata* from Mar Piccolo, Taranto, *Mar. Chem.*, 58 (1997) 319–325.
- [54] N.A.A. Nazri, R.S. Azis, H.C. Man, A.H. Shaari, N.M. Saidu, I. Ismail, Equilibrium studies and dynamic behavior of cadmium adsorption by magnetite nanoparticles extracted from mill scales waste, *Desal. Water Treat.*, 171 (2019) 115–131.
- [55] Z. Aksu, G. Dönmez, A comparative study on the biosorption characteristics of some yeasts for Remazol Blue reactive dye, *Chemosphere*, 50 (2003) 1075–1083.
- [56] Z. Yaneva, B. Koumanova, Comparative modeling of mono- and dinitrophenols sorption on yellow bentonite from aqueous solutions, *J. Colloid Interface Sci.*, 293 (2006) 303–311.
- [57] C.H. Giles, T.H. MacEwan, S.N. Nakhwa, D. Smith, Studies in adsorption. Part XI. A system of classification of solution adsorption isotherms, and its use in diagnosis of adsorption mechanisms and in measurement of specific surface areas of solids, *J. Chem. Soc.*, 973 (1960) 3973–3993.
- [58] H.B. Senturk, D. Ozdes, C. Duran, Biosorption of Rhodamine 6G from aqueous solutions onto Almond shell (*Prunus dulcis*) as a low-cost biosorbent, *Desalination*, 252 (2010) 81–87.
- [59] F. Bessaha, K. Marouf-Khelifa, I. Batonneau-Gener, A. Khelifa, Characterization and application of heat-treated and acid-leached halloysites in the removal of malachite green: adsorption, desorption, and regeneration studies, *Desal. Water Treat.*, 57 (2016) 14609–14621.
- [60] M. Saeed, M. Munir, M. Nafees, S.S.A. Shah, H. Ullah, A. Waseem, Synthesis, characterization and applications of silylation based grafted bentonites for the removal of Sudan dyes: isothermal, kinetic and thermodynamic studies, *Microporous Mesoporous Mater.*, 291 (2020) 1096–1097.